An Environmentally Sensitive Phase Map of Titania Nanocrystals

Amanda S. Barnard[†,*] and Huifang Xu[‡,*]

[†]School of Chemistry, The University of Melbourne, Parkville, 3010, Australia, and [‡]Department of Geology and Geophysics, and Materials Science Program, University of Wisconsin—Madison, Madison, Wisconsin 53706

ABSTRACT The incorporation of more experimentally relevant parameters into theoretical descriptions of nanomaterials is important for our understanding of the stability of nanostructures in different chemical environments. Using a size-, shape-, and temperature-dependent thermodynamic model we have generated the first phase map for anatase and rutile nanocrystals, that includes both the equilibrium shape and the affects of surface chemistry. The calculated phase map indicates that the equilibrium boundary between anatase and rutile nanocrystals is surface charge chemistry dependent, which relates to both their formation and postsynthesis environments.

KEYWORDS: titania · nanocrystal · surface chemistry · phase diagram · theory · simulation · TEM

Nanostructures of titania (TiO_2) are of considerable scientific interest, because of their superior performance in a range of advanced photochemical applications. In addition to the finite size affects, it has been found that the crystalline phase (anatase or rutile) and the shape of individual nanocrystals are also critical parameters in determining their photocatalytic efficiency,[1,2] and overall suitability for particular applications.[3−5] Recent studies have demonstrated remarkable control over the morphology of titania nanostructures;[6] however, this requires very specific synthesis conditions which are dissimilar to the environment in which these materials will ultimately be used and the (greater) natural environment with which they are likely to interact. Predicting the effect changing the chemical environment will have upon titania nanostructures is highly desirable, but the incorporation of more environmentally relevant parameters into theoretical descriptions of nanomaterials is not trivial.

In general it is well-known that rutile is the thermodynamically stable phase of TiO_2 under ambient conditions at the macroscale,[7] and that anatase is the thermodynamically stable phase at the nanoscale.[8,9] A number of authors[10−13] have shown that the synthesis of nanocrystalline TiO_2 consistently resulted in anatase nanocrystals, which transformed to rutile upon reaching a particular size.[14] The size range of the anatase-to-rutile phase transition for hydrothermal samples (at ~650−800 K) has been predicted to be in the range of 11.4−17.6 nm.[10] However, anatase nanocrystals are often observed over this size[1,9,15,16] depending upon the temperature and surface chemistry. From experiment, it usually found that titania surfaces includes >TiOH surface hydroxyl groups,[16−22] and under neutral pH conditions the surfaces are terminated with H_2O (either as molecular H_2O or as dissociated $OH^- + H^+$) or OH.[9,17,18] These terminations are more commonly observed than alternative combinations of O and H,[23] and are most likely to be present on the surface when titania particles are exposed to pH neutral atmospheric conditions.[17,18]

Although the size-dependent phase boundary between anatase and rutile has been calculated a number of times over the past decade, previous studies do not allow for the dynamic variations in nanomorphology as a function of temperature,[11,23,24] and rarely include the important influence of surface adsorbates.[23] There is no doubt that this has been partially responsible for some discrepancy between theoretical and experimental results reported in the literature. To begin addressing these issues, and incorporating more experimentally (and environmentally) relevant parameters into theoretical descriptions, we have used thermodynamic modeling to generate the first complete size-temperature phase map for anatase and rutile nanocrystals in the presence of passivating surface groups.

*Address correspondence to amanda.barnard@unimelb.edu.au, hfxu@geology.wisc.edu.

Received for review July 15, 2008 and accepted October 21, 2008.

Published online November 7, 2008. 10.1021/nn800446w CCC: $40.75

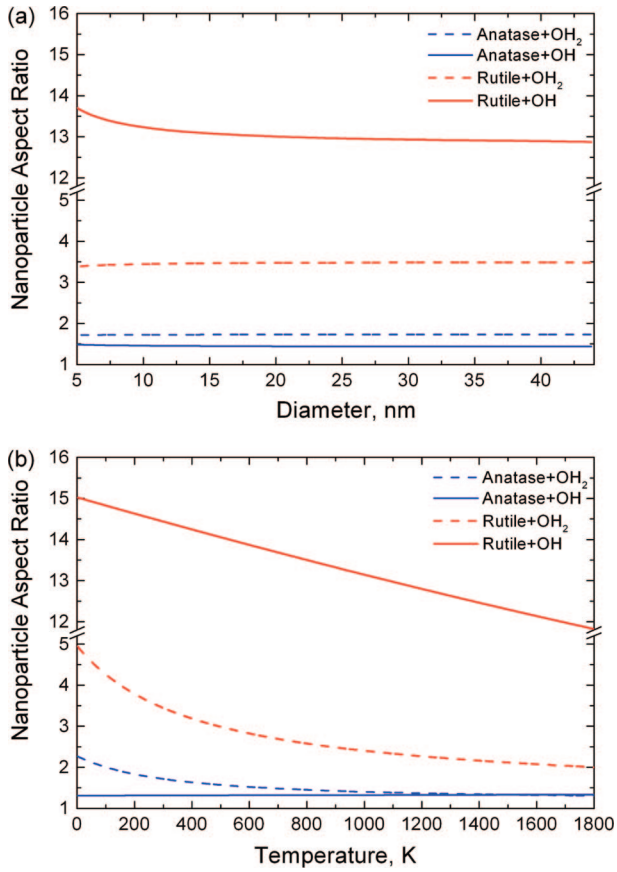

Figure 1. The size and temperature dependence of the equilibrium aspect ratio of OH_2- and OH-terminated anatase and rutile nanocrystals where (a) the temperature is fixed at 300 K, and (b) the average diameter is fixed at 10 nm.

In general, a phase map is a two-dimensional graphical representation of chemical equilibrium, indicating stability of solid polymorphs at a given temperature, composition, and/or pressure. Nanoscale phase maps have another axis representing the size (in this case the average diameter D), but are more complicated since the surface (rather than bulk) effects may dominate. Therefore, our modeling uses the equilibrium shape at each size (D) and temperature (T), and includes an optimization of the morphology of rutile nanocrystals for the first time.

DISCUSSION OF RESULTS

Equilibrium Nanocrystal Shapes. We have begun by using a well-tested general shape-dependent thermodynamic multiscale model, and the consistent set of computational results reported elsewhere,[36,40] to determine the equilibrium morphology (shape) of both anatase and rutile. This is achieved by optimizing the polyhedral shape so as to minimize the total free energy as a function of size for a range of temperatures. Equivalently, this may also be achieved by optimizing the shape to minimize the total free energy as a function of temperature, for a range of sizes. To illustrate how the nanocrystal shape may change during this type of geometry optimization, Figure 1 shows the total aspect ratio[41] of anatase and rutile particles with OH_2- and OH-terminated surfaces. In Figure 1a the temperature is fixed at 300 K (while the average diameter is varied), and in Figure 1b the average diameter is fixed at 10 nm (while the temperature is varied). Although the shape of anatase nanocrystals has been examined previously,[38] this is the first time that the equilibrium shape of rutile nanocrystals has been determined.

Predicted Phase Map. From each optimization we have compared the values of $T_m(D)$ and $G_x(T)$ for both anatase and rutile, and mapped the lowest energy phase in $\langle D, T \rangle$ space. Since there is a volumetric disparity between anatase and rutile, due to the differences in ρ_x, this comparison was performed as a function of the number of TiO_2 formula units. Once the critical number of formula units was determined (in each case) it was then converted to the equivalent anatase nanocrystal diameter. These results are shown in Figure 2, where we can see that the position of the anatase-to-rutile solid−solid phase transition line differs depending on the type of adsorbed groups. In the region between the OH- and OH_2-terminated, the surfaces may be terminated with combinations of both groups, depending on the solution environment. This is effectively a coexistence region where the relative stability of anatase and rutile will be sensitive to the surface chemistry, and structural transitions will be coupled with adsorption−desorption reactions, as well as shape-transitions. In general the phase diagram indicates that an increase in H favors rutile stability (increasing the rutile stability field). When examining Figure 2 we are reminded that, in addition to finite temperatures, these calculations include the optimization of the rutile morphology, both of which were not included in previous work.[23] These new inclusions make the theory more consistent to real experiments, and allows for the direct comparisons with experiments needed for verification.

Comparison with Experiment. To verify the important features of this phase map, we have first examined the surface chemistry under neutral conditions using Fourier transform infrared (FTIR) spectroscopy. We can see from the results in Figure 3 the peak at ~1650−1630 cm^{-1} due to the bending mode between two H atoms of H_2O (in pure water) or $>OH_2$ of the titania surface group. The large difference (~20 cm^{-1}) of the peak positions indicate that the peak for this titania sample is not just from neutral water, but from surface $>OH_2$ groups with different bending frequency (or energy). The broad peak at ~3000−3700 cm^{-1} is due to the stretching mode between O and H, which could occur in both H_2O and OH groups. Furthermore, the large absorbance peak for the anatase dominated titania sample indicates that there are >OH surface groups in addition to $>OH_2$ surface groups. These results are entirely consistent with the results of Soria *et al.*[25]

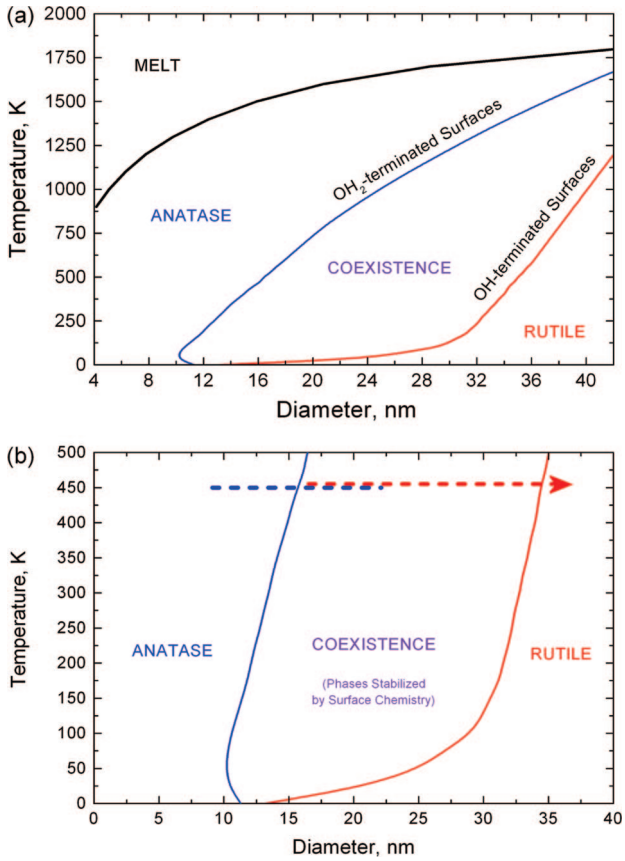

Figure 2. The ⟨*D*, *T*⟩ phase map of titania, based on first principles calculations and melting enthalpies form experiment: (a) the solid−solid phase transition lines for nanocrystals with OH_2- and OH-terminated surfaces and the coexistence region where the relative stability depends on the type of adsorbed groups, and (b) the low temperature and size regime with the size range of experimental observations at 180 °C and 0.2 M HCl marked (anatase in blue, and rutile in red). Identification of individual anatase and rutile nanocrystals are base on their periodicties of lattice fringes in HR-TEM images. The diameter refers to the anatase phase.

Previously it has been found during hydrothermal synthesis results of anatase and rutile nanocrystals at 180 °C in different acidity solutions shows that solutions with high acidity (*i.e.*, more $>OH_2$ surface group and less >OH group) favor rutile formation and stability.[26,27] Titania formed in solutions with 0.5 M HCl or higher produce almost entirely pure rutile nanocrystals.[27] The size of small rutile crystals in these experiments was measured at approximately 14−18 nm (see Figure 4a). When the solutions contain low concentration of HCl (0.4 M or lower), both rutile and anatase nanocrystals formed[27] (as we can see from Figure 4b), and it was concluded that low acidity and pure water solutions favor anatase nanocrystal formation. On the basis of recent high temperature titration and surface protonation model, the rutile surface in such an acidic solution will be dominated by $>OH_2$ surface group and displays net positive surface charge at 180 °C.[28] Although there is no high-temperature titration data for anatase, its surface protonation behavior could be similar to that of rutile, because both polymorphs have similar point-of-zero-charge pH values (pH_{pzc}), and $Ti-O_6$ octahedra in their structure.[32]

There has been considerable data gathered on titania nanocrystals in recent years, and a comprehensive review of all of the reported experimental results is beyond the scope of this article. However, an examination of the modest list of references included here reveal that the anatase-to-rutile transformation is routinely found to occupy this region of the phase map, when grown using hydrothermal synthesis. Almost a decade ago it was shown that acidic solutions favor rutile formation,[29,30] whereas, basic conditions favors anatase formation,[31] but because the crystal sizes were determined based on bulk X-ray powder diffraction (not individual nanocrystals measured using TEM), it is very difficult to quantify the size boundary or size overlap zone. Direct comparison with theory and experiment is further complicated by the fact that studies that do use TEM show that titania samples present a variation in size and shape, some of which is beyond that which is predicted in Figures 1 and 2. In Figure 4a for instance, the length of the rutile crystals range from 50 to 200 nm. It is therefore pertinent to remind readers that the theoretical model use here is a thermodynamic model, and a phase map is principally a thermodynamic construct, whereas kinetic considerations are also known to be important in determining the eventual size, shape, and solid phase of titania nanocrystals.[33,34] This phase map is therefore not able to predict the cases where the shapes deviate significantly from equilibrium, but it can offer guide as to how unstable kinetically grown nonequilibrium shapes are expected to be.

The solid−liquid transition line is more difficult to validate. Obtaining higher temperatures (over 1000 K) and true equilibrium simultaneously in the

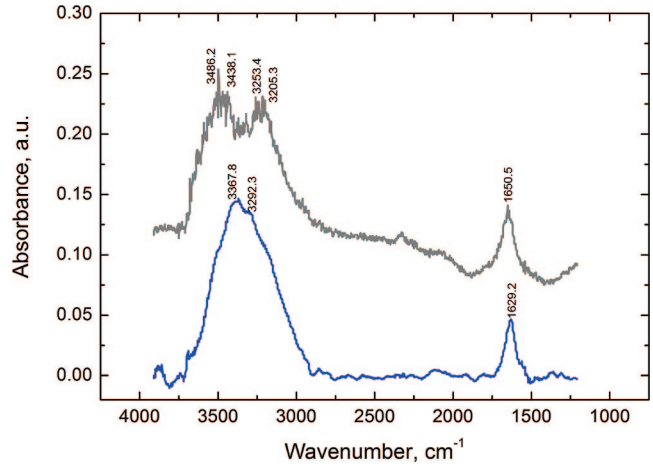

Figure 3. FTIR spectra from pure water (upper gray spectrum) and anatase dominated titania (lower blue spectrum) in neutral condition. The FTIR spectra indicate both >OH and $>OH_2$ groups occur on the titania surface.

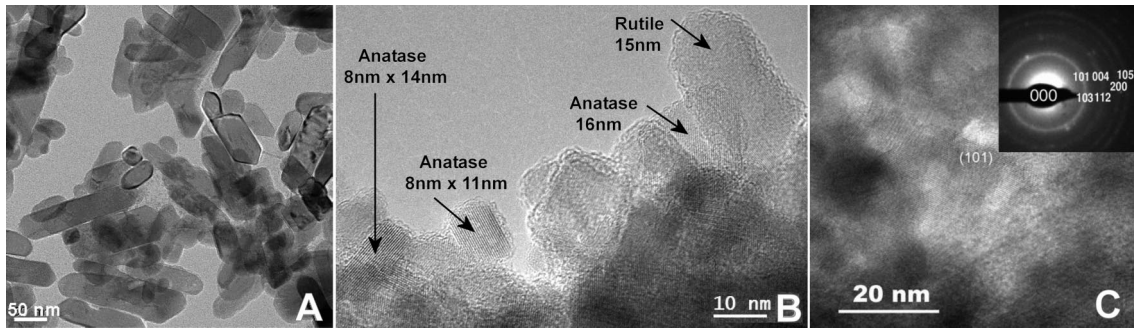

Figure 4. (A) TEM image showing rutile nanocrystals formed in 0.5 M HCl solution at 180 °C. Small rutile crystals have diameters of 14−18 nm; (B) TEM image showing rutile and anatase nanocrystals formed in 0.2 M HCl solution at 180 °C; (C) High-resolution TEM images showing anatase nanocrystals in the fresh basalt glass. A *ca.* 25 nm size crystal is labeled with (101) due to its (101) lattice fringes. Inserted electron diffraction pattern (at up-right corner) is from the cluster only. The diffraction pattern from neighboring basalts glass displays very broad and diffuse diffraction ring (not shown).

laboratory is challenging, but is achieved easily in nature and preserved geologically. With the benefit of time, natural nanocrystals are able to adopt their equilibrium structure subject to environmental conditions. We have observed anatase nanocrystal clusters in a young and fresh basalt glass layer in the McKinney Butte Basalt of Snake River Group Basalt in the Snake River area of Idaho.[35] Figure 4c shows a TEM micrograph of these samples, showing the (101) lattice fringes of the Fe-bearing anatase nanocrystals in the fresh basalt glass. Although the exact condition for the anatase formation in these layers is not certain, it is clear that these anatase nanocrystals formed in a hot environment of basalt rock due to the presence of Fe(III) in solid solution state, which supports that anatase is the thermodynamically stable phase for titania nanocrystals at high temperatures. In general, solubility of Fe(III) in either rutile and anatase is very low, and one expects that such a small amount of Fe in these natural anatase nanocrystals will not influence the anatase stability with respect to rutile. While this may not be an ideal comparison, due to the presence of Fe impurities which are known to affect the stability of the crystalline faces, it does provide a very unique insight that cannot be provided by any other data (even if it were available).

CONCLUSION

To conclude, we suggest that when taken in combination with the changing thermal conditions, moving from OH_2- and OH-terminated surfaces constitutes a fundamental change in chemical environment. Recall that a phase map is a graphical representation of chemical equilibrium, which at the nanoscale must include the characteristic surface chemistry. It is anticipated that these results will help to explain the sensitivity of titania nanocrystals stability to size, temperature, and surface chemistry, and offer a more complete theoretical framework for future studies. The next issue to be addressed is the adequate inclusion of surface charge, since many titania nanocrystals are synthesized using organic compounds, and the influence of interactions with organic molecules. These are both important parameters in determining the agglomeration behavior and stability of real samples. The ultimate aim of our future work will be to continue to develop an understanding of the quantitative relationship among phase stabilities, crystal surface speciation, and solution chemistry.

METHODS

Theoretical Method. The modeling was carried out using a shape-dependent thermodynamic model based on a geometric summation of the Gibbs free energy[36,37] which has previously been successfully used to examine the shape of titania.[23,38] The version of the model used here is applicable specifically to isolated, defect-free structures:

$$G_x(T) = \Delta_f G_x^o(T) + \frac{M}{\rho_x}\left(1 - \frac{2\Sigma_i f_i \sigma_{xi}^y(T)}{B_0 R_{av}} + \frac{P_{ex}}{B_0}\right)[q\sum_i f_i \gamma_{xi}^y(T)] \quad (1)$$

where M is the molar mass and ρ is the density. Unlike other models used to describe the free energy of materials, that model specifically accounts for the polyhedral shapes of nanocrystals (as well as the finite size) *via* the sum over the individual contribution from the exposed surface facets i. The volume dilation induced by the isotropic surface stresses σ_{xi} and external pressure P_{ex} is also included *via* the Laplace−Young formalism,[37] using the bulk modulus B_0 (of phase x), and the average particle radius R_{av} calculated using a spherical approximation. In all cases atmospheric external pressure has been assumed. As described in reference 11, the standard free energy of formation $\Delta_f G_x^o(T)$ (with x = anatase and rutile) is described using a regression representation widely used in phase diagram calculations and data from the JANAF tables.[39] More information on the model may be found in references 23 and 37.

This leaves the temperature-dependent specific surface energies and isotropic surface stresses. In the present study, we examine the case of OH_2- and OH-terminated surfaces. The structure and energy of the OH_2- and OH-terminated {110}, {100}, {011}, and {001} surfaces of both anatase and rutile have been described in great detail elsewhere.[40] Briefly, the specific surface energies were calculated from the energy per stoichiometric unit of the bulk, μ_{TiO_2}, and the total energy of the surface, $E_{xi}(N_{TiO_2})$, slabs using the expression

$$\gamma^{y}_{xi} = \frac{1}{2A_{xi}}(E_{xi}(N_{TiO_2}) - N_{TiO_2}\mu_{TiO_2} - N_y\mu_y) \quad (2)$$

where A is the area of the surface and N_{TiO_2} is the number of TiO_2 units in the (stoichiometric) cell. Here, μ_y is the chemical potential of the adsorbates y, and N_y is the total number of adsorbate molecules per unit A.[40] The chemical potential μ_y was constructed from the chemical potentials of water and hydrogen,

$$\mu_{OH_2} = E_{OH_2} + \frac{h\nu_{OH_2}}{2} + k_B T\left[\ln\left(\frac{PV}{k_B T}\right)\right] \quad (3)$$

$$\mu_{OH} = \mu_{OH_2} - \frac{1}{2}\left(E_{H_2} + \frac{h\nu_{H_2}}{2} + k_B T\left[\ln\left(\frac{PV}{k_B T}\right)\right]\right) \quad (4)$$

so that water and hydroxyl adsorbates are in mutual equilibrium, within the stability fields of the chemical potential reservoir, as described in reference 40. Of course, k_B is Boltzmann's constant, T, P, and ν are the temperature, pressure, and sum of the vibrational frequencies in the reservoir, and V is the quantum volume,[42]

$$V = \left(\frac{h^2}{2\pi m k_B T}\right)^{3/2} \quad (5)$$

Furthermore, since $\sigma = \partial G/\partial A$ the temperature dependence of σ^{y}_{xi} is assumed consistent with γ^{y}_{xi}, and the same slope is applied. The energetic terms in the chemical potentials and the $T = 0$ coefficients for the surface energies and isotropic surfaces stresses have been previously calculated from first principles, and are listed in references 23 and 40.

Finally, the classical definition of the size dependent melting temperature T_m is expressed in terms of the bulk melting temperature $T_{m,\infty}$, such that

$$\frac{T_m}{T_{m,\infty}} = 1 + \frac{A_t(\gamma_l - \gamma_s)}{V_t \Delta H_{m,\infty}} \quad (6)$$

where A_t is the total surface area, V_t is the total volume, γ_l is the surface energy of the liquid, and $\Delta H_{m,\infty}$ is the melting enthalpy. This formalism has recently been shown to be applicable to titania nanocrystals over ~2 nm by Guisbiers *et al.*,[24] however by recognizing that A_t/V_t is the definition of q (which changes with both size and temperature during the morphological optimization), a more general description of the size and shape dependent melting temperature for nanocrystals in equilibrium is given by

$$T_m(D) = T_{m,\infty}\left[1 + q(T,D)\frac{\gamma_l - \Sigma f_i \gamma^{y}_{xi}(T)}{\Delta H_{m,\infty}}\right] \quad (7)$$

This may be calculated for any shape (enclosed by the surfaces i) with surface to volume ratio q, using the bulk melting temperatures, the surface energy of the liquid,[43] and the enthalpy of melting from experiment.[44] It is important to point out that since q is now expressed as $q(T, D)$, $T_m(D)$ is obtained by self-consistently solving for D when $T = T_m(D)$ during each optimization of $q(T, D)$ (*i.e.*: during the morphological optimization to minimize the total free energy of the system).

Fourier Transform Infrared (FTIR) Spectroscopy. The FTIR spectra were recorded using infrared radiation from the synchrotron ring at the University of Wisconsin Madison Synchrotron Radiation Center. The FTIR spectrometer is a model Magna 560 made by Thermo Electron Corporation. It is capable of a resolution of up to 0.01 cm^{-1} and is coupled to a Nicolet infrared microscope (Thermo Electron Corporation) with a programmable sample stage and redundant aperturing. The spectra were recorded in the reflectance mode using a 32X all reflective objective lens (numerical aperture of 0.58). The FTIR spectrometer is internally calibrated using a HeNe laser.

Acknowledgment. Experimental study of the anatase and rutile nanocrystals was supported by NSF (EAR-0810150). Computational resources for this project have been supplied by Pacific Northwest National Laboratory Molecular Science Computing Facility. We would like to thank Larry Curtiss at ANL for his support and for useful discussions and Robert Julian of University of Wisconsin Madison Synchrotron Radiation Center for assisting FTIR analyses.

REFERENCES AND NOTES

1. Testino, A.; Bellobono, I. R.; Buscaglia, V.; Canevali, C.; D'Arienzo, M.; Polizzi, S.; Scotti, R.; Morazzoni, F. Optimizing the Photocatalytic Properties of Hydrothermal TiO_2 by the Control of Phase Composition and Particle Morphology. A Systematic Approach. *J. Am. Chem. Soc.* **2007**, *129*, 3564–3575.
2. Balázs, N. Mogyorósi, K. Srankó, D. F. Pallagi, A. Alapi, T. Oszkó, A. Dombi, A. Sipos, P. The Effect of Particle Shape on the Activity of Manocrystalline TiO_2 Photocatalysts in Phenol Decomposition, *Appl. Catal., B*, doi:10.1016/j.apcatb.2008.04.018.
3. Rajh, T.; Nedeljkovic, J. M.; Chen, L. C.; Poluektov, O.; Thurnauer, M. C. Improving Optical and Charge Separation Properties of Nanocrystalline TiO_2 by Surface Modification with Vitamin C. *J. Phys. Chem. B* **1999**, *103*, 3515–3519.
4. Zhang, H.; Penn, R. L.; Hamers, R. J.; Banfield, J. F. Enhanced Adsorption of Molecules on Surfaces of Nanocrystalline Particles. *J. Phys. Chem. B* **1999**, *103*, 4656–4662.
5. Bullen, H.; Garrett, S. TiO_2 Nanoparticle Arrays Prepared Using a Nanosphere Lithography Technique. *Nano Lett.* **2002**, *2*, 739–745.
6. Satoh, N.; Nakashima, T.; Kamikura, K.; Yamamoto, K. Quantum Size Effect in TiO_2 Nanoparticles Prepared by Finely Controlled Metal Assembly on Dendrimer Templates. *Nat. Nanotechnol.* **2008**, *3*, 106–111.
7. Muscat, J.; Swamy, V.; Harrison, N. M. First-Principles Calculations of the Phase Stability of TiO_2. *Phys. Rev. B* **2002**, *65*, 224112–224126.
8. Ranade, M. R.; Navrotsky, A.; Zhang, H. Z.; Banfield, J. F.; Elder, S. H.; Zaban, A.; Borse, P. H.; Kulkarni, S. K.; Doran, G. S.; Whitfield, H. J. Energetics of Nanocrystalline TiO_2. *Proc. Natl. Acad. Sci. U.S.A.* **2002**, *99*, 6476–6481.
9. Levchenko, A. A.; Li, G.; Boerio-Goates, J.; Woodfield, B. F.; Navrotsky, A. TiO_2 Stability Landscape: Polymorphism, Surface Energy, and Bound Water Energetics. *Chem. Mater.* **2006**, *18*, 6324–6332.
10. Gribb, A. A.; Banfield, J. F. Particle Size Effects on Transformation Kinetics and Phase Stability in Nanocrystalline TiO_2. *Am. Mineral.* **1997**, *82*, 717–729.
11. Zhang, H.; Banfield, J. F. Thermodynamic Analysis of Phase Stability of Manocrystalline Titania. *J. Mater. Chem.* **1998**, *8*, 2073–2076.
12. Navrotsky, A. Thermochemistry of Nanomaterials. In *Nanoparticles and the Environment, Reviews in Mineralogy Geochemistry*; Banfield, J. F., Navrotsky, A., Eds.; Mineralogical Society of America: Washington, DC, 2001; Vol. 44.
13. Zhang, H.; Finnegan, M.; Banfield, J. F. Preparing Single-Phase Nanocrystalline Anatase from Amorphous Titania with Particle Sizes Tailored by Temperature. *Nano Lett.* **2001**, *1*, 81–84.
14. Navrotsky, A. Energetics of Nanoparticle Oxides: Interplay Between Surface Energy and Polymorphism. *Geochem. Trans.* **2003**, *4*, 34–37.
15. Li, W.; Ni, C.; Lin, H.; Huang, C. P.; Ismat Shaha, S. Size Dependence of Thermal Stability of TiO_2 Nanoparticles. *J. Appl. Phys.* **2004**, *96*, 6663–6668.
16. Saponjic, Z. V.; Dimitrijevic, N.; Tiede, D.; Goshe, A.; Zuo, X.; Chen, L.; Barnard, A. S.; Zapol, P.; Curtiss, L. A.; Rajh, T. Shaping Nanometer-scale Architecture Through Surface Chemsitry. *Adv. Mater.* **2005**, *17*, 965–971.
17. Diebold, U. The Surface Science of Titanium Dioxide. *Surf. Sci. Rep.* **2003**, *48*, 53–229.

18. Hoffmann, M. R.; Martin, S. T.; Choi, W.; Bahnemann, D. W. Environmental Applications of Semiconductor Photocatalysis. *Chem. Rev.* **1995**, *95*, 69–96.
19. Thurnauer, M. C.; Rajh, T.; Tiede, D. M. Surface Modification of TiO_2: Correlation Between Structure, Charge Separation, and Reduction Properties. *Acta Chem. Scand.* **1997**, *51*, 610–618.
20. Nakaoka, Y.; Nosaka, Y. ESR Investigation into the Effects of Heat Treatment and Crystal Structure on Radicals Produced Over Irradiated TiO_2 Powder. *J. Photochem. Photobiol. A* **1997**, *110*, 299–305.
21. Szczepankiewicz, S. H.; Moss, J. A.; Hoffmann, M. R. Electron Traps and the Stark Effect on Hydroxylated Titania Photocatalysts. *J. Phys. Chem. B* **2002**, *106*, 7654–7658.
22. Kasuga, T.; Hiramatsu, M.; Hoson, A.; Sekino, T.; Niihara, K. Titania Nanotubes Prepared by Chemical Processing. *Adv. Mater.* **1999**, *11*, 1307–1311.
23. Barnard, A. S.; Curtiss, L. A. Prediction of TiO_2 Nanoparticle Phase and Shape Transitions Controlled by Surface Chemistry. *Nano Lett.* **2005**, *1*, 1261–1266.
24. Guisbiers, G.; Van Overschelde, O.; Wautelet, M. Theoretical Investigation of Size and Shape Effects on the Melting Temperature and Energy Bandgap of TiO_2 Nanostructures. *Appl. Phys. Lett.* **2008**, *92*, 103121–103123.
25. Soria, J.; Sanz, J.; Sobrados, I.; Coronado, J. M.; Maira, A. J.; Hernandez-Alonso, M. D.; Fresno, F. FTIR and NMR Study of the Adsorbed Water on Nanocrystalline Anatase. *J. Phys. Chem. C* **2007**, *111*, 10590–10596.
26. Finnegan, M. P.; Zhang, H.; Banfield, J. F. Phase Stability and Transformation in Titania Nanoparticles in Aqueous Solutions Dominated by Surface Energy. *J. Phys. Chem. C* **2007**, *111*, 1962–1968.
27. Yeredla, R. R.; Xu, H. An Investigation of Nanostructured Rutile and Anatase Plates for Improving the Photosplitting of Water. *Nanotechnology* **2008**, *19*, 055706−055715.
28. Machesky, M. L.; Wesolowski, D. J.; Ridley, M. K.; Palmer, D. A.; Rosenqvist, J.; Lvov, S. N.; Fedkin, M.; Předota, M.; Vlcek, L. The Protonation Behavior of Metal Oxide Surfaces to Hydrothermal Conditions. *ECS Transactions* **2008**, *11*, 151–166.
29. Wang, C.-C.; Ying, J. Y. Sol-Gel Synthesis and Hydrothermal Processing of Anatase and Rutile Titania Nanocrystals. *Chem. Mater.* **1999**, *11*, 3113–3120.
30. Yang, J.; Mei, S.; Ferreira, J. M. F. Hydrothermal Synthesis of Nanosized Titania Powders: Influence of Peptization and Peptizing Agents on the Crystalline Phases and Phase Transitions. *J. Am. Ceram. Soc.* **2000**, *83*, 1361–1368.
31. Yanagisawa, K.; Ovenstone, J. Crystallization of Anatase from Amorphous Titania Using the Hydrothermal Technique: Effects of Starting Material and Temperature. *J. Phys. Chem. B* **1999**, *103*, 7781–7787.
32. Schindler, P. W.; Stumm, W. The Surface Chemistry of Oxides, Hydroxides, and Oxide Minerals. In *Aquatic Surface Chemistry*; Stumm W., Ed.; Wiley-Interscience: New York, 1987; pp 83−110.
33. Zhang, H.; Banfield, J. F. New Kinetic Model for the Nanocrystalline Anatase-to-Rutile Transformation Revealing Rate Dependence on Number of Particles. *Am. Mineral.* **1999**, *84*, 528–535.
34. Zhang, H.; Banfield, J. F. Size Dependence of the Kinetic Rate Constant for Phase Transformation in TiO_2 Nanoparticles. *Chem. Mater.* **2005**, *17*, 3421–3425.
35. Gilleman, V. S.; Kauffman, J. D.; Othberg, K. L. *Thousand Springs Quadrangle, Gooding and Twin Falls Counties, Idaho*; Idaho Geological Survey: University of Idaho, Moscow, ID, 2005.
36. Barnard, A. S.; Zapol, P. A Model for the Phase Stability of Arbitrary Nanoparticles as a Function of Size and Shape. *J. Chem. Phys.* **2004**, *121*, 4276–4283.
37. Barnard, A. S. A Thermodynamic Model for the Shape and Stability of Twinned Nanostructures. *J. Phys. Chem. B* **2006**, *110*, 24498–24504.
38. Barnard, A. S.; Zapol, P. Predicting the Energetics, Phase Stability, and Morphology Evolution of Faceted and Spherical Anatase Nanocrystals. *J. Phys. Chem. B* **2004**, *108*, 18435–18440.
39. Chase, M. W.; Davies, C. A.; Downey, J. R.; Frurip, D. J.; McDonald, R. A.; Syverud, A. N. *J. Phys. Chem. Ref. Data* **1985**, *14*, 1680.
40. Barnard, A. S.; Zapol, P.; Curtiss, L. A. Anatase and Rutile Surfaces with Adsorbates Representative of Acidic and Basic Conditions. *Surf. Sci.* **2005**, *582*, 173–188.
41. Defined as the ratio of the average diameter of the nanocrystal in the *a*- and *b*-plane and the total length of the nanocrystal along the *c*-axis.
42. Rushbrook, G. S. *Introduction to Statistical Mechanics*; Clarendon Press: Oxford, U.K., 1957.
43. Li, Y. L.; Ishigaki, T. Thermodynamic Analysis of Nucleation of Anatase and Rutile from TiO_2 Melt. *J. Cryst. Growth* **2002**, *242*, 511–516.
44. Martinssen, W.; Walimont, H. *Springer Handbook of Condensed Matter and Materials Data*; Springer: Berlin, 2005.